ACS ENGINEERING Au
AN OPEN ACCESS JOURNAL OF THE AMERICAN CHEMICAL SOCIETY

pubs.acs.org/engineeringau
Article

Upscaling Plasma-Based CO_2 Conversion: Case Study of a Multi-Reactor Gliding Arc Plasmatron

Published as part of ACS Engineering Au virtual special issue "Sustainable Energy and Decarbonization".

Colin O'Modhrain,[§] Georgi Trenchev,[§] Yury Gorbanev,[*,§] and Annemie Bogaerts[§]

Cite This: *ACS Eng. Au* 2024, 4, 333−344
Read Online

ACCESS | Metrics & More | Article Recommendations | Supporting Information

ABSTRACT: Atmospheric pressure plasmas have shifted in recent years from being a burgeoning research field in the academic setting to an actively investigated technology in the chemical, oil, and environmental industries. This is largely driven by the climate change mitigation efforts, as well as the evident pathways of value creation by converting greenhouse gases (such as CO_2) into useful chemical feedstock. Currently, most high technology readiness level (TRL) plasma-based technologies are based on volumetric and power-based scaling of thermal plasma systems, which results in large capital investment and regular maintenance costs. This work investigates bringing a quasi-thermal (so-called "warm") plasma setup, namely, a gliding arc plasmatron, from a lab-scale to a pilot-scale capacity with an increase in throughput capacity by a factor of 10. The method of scaling is the parallelization of plasmatron reactors within a single housing, with the aim of maintaining a warm plasma regime while simultaneously improving build cost and efficiency (compared to separate reactors operating in parallel). Special attention is also given to the safety and control features implemented in the setup, a key component required for integration into industrial systems. The performance of the multi-reactor gliding arc plasmatron (MRGAP) reactor is investigated, focusing on the influence of flow rate and the number of active reactors. The location of active reactors was deemed to have a negligible effect on the monitored metrics of conversion, energy efficiency, and energy cost. The optimum operating conditions were found to be with the most active reactors (five) at the highest investigated flow rate (80 L/min). Analysis of results suggests that an optimum conversion (9%) and plug power-based energy efficiency (19%) can be maintained at a specific energy input (SEI) around 5.3 kJ/L (or 1 eV/molecule). The concept of parallelization of plasmatron reactors within a singular housing was demonstrated to be a viable method for scaling up from a lab-scale to a prototype-scale device, with performance analysis suggesting that increasing the power (through adding more reactor channels) and total flow rate, while maintaining an SEI around 5.3 or 4.2 kJ/L, i.e., 1.3 or 1 eV/molecule (based on plug power and plasma-deposited power, respectively), can result in increased conversion rate without sacrificing absolute conversion or energy efficiency.

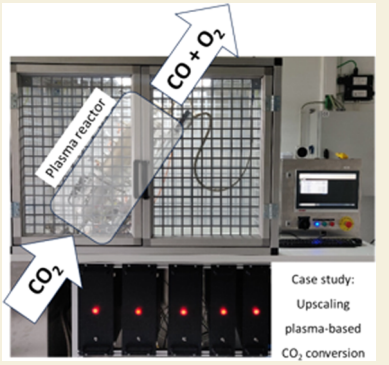

KEYWORDS: *carbon dioxide, gliding arc plasma, upscaling, energy efficiency, conversion, plasmolysis, electrification of chemical industry*

1. INTRODUCTION

In the past decades, global urbanization and industrialization have led to increased energy demand. Currently, most of the world's energy comes from fossil fuels, which are not only predicted to be depleted by the mid-21st century[1] but are also responsible for the climate change due to the concomitant emissions of CO_2. In light of climate change and the efforts to adapt to it, the developed world is in the middle of a massive-scale energy transition from fossils to renewable energy sources. This transition involves replacing or supplementing fossil fuels with clean and renewable alternatives such as solar, wind, hydroelectric, and geothermal energy. These sources generate electricity with significantly lower carbon emissions, making them a critical part of efforts to reduce the environmental impact of energy production.[2]

There have been long-lasting debates on which sectors would be impacted the most by this energy transition phase.[3] It is clear that matching the flexibility of renewable sources is the key to a successful transition. This is feasible for the chemical industry and will lead to significant positive impacts on global decarbonization.

Plasma-based technology has been identified as one of the most viable pathways for electrification of the chemical industry, attributed primarily to the technology compatibility

Received: October 31, 2023
Revised: January 30, 2024
Accepted: January 31, 2024
Published: February 14, 2024

Table 1. Summarized Recent Advances in CO_2 Plasmolysis[a]

#	plasma reactor	pressure (atm)	feed CO_2 flow rate (L/min)	specific energy input[b] (kJ/L)	CO_2 conversion		energy[b]		refs
					extent (%)	rate (g/h)	cost (MJ/mol)	efficiency (%)	
1	microwave with post-plasma nozzle	0.9	5	18.0	35.0	192	1.2	25	24
2	microwave with cooled effluent	1	10	16.5	35.0	384	1.1	26	25
3	microwave with post-plasma nozzle	0.7	15	5.2	13.0	216	1	31	26
4	microwave	0.9	100	1.4	2.7	318	1.3	24	8
5[c]	DC atmospheric pressure glow discharge	1	1	3.9	8.2	12	1.1	25	27
6	pulsed dielectric barrier discharge	1	0.02	154.7	51.4	1	7.2	4	28
7	dielectric barrier discharge with packed dielectric	1	0.03	4.0	9.3	<1	1	12	29
8	AC spark discharge	1	0.03	15.2	10.3	<1	3.3	8	30
9[d]	AC gliding arc plasmatron with carbon bed	1	10	3.2	7.6	84	1	28	31
10	DC gliding arc plasmatron	1	10	3.9	9.5	102	1	30	9
11	DC multi-reactor gliding arc plasmatron	1	80	5.3[e] (4.2[b])	8.7	777	1.5[e] (1.2[b])	20[e] (24[b])	this work

[a]For entry 11, the values of SEI, energy cost, and energy efficiency are shown for both the plug power and the plasma power. [b]The values are based on the plasma-deposited power only. [c]The results are shown for a single-pass reactor. [d]Single-pass reactor without enhancement from an added carbon bed. [e]These values are based on the total (i.e., plug-to-product) power.

with intermittent renewable energy resources.[4−7] Plasma offers a fully electrified gas conversion pathway without the need for special catalysts or rare materials. Moreover, the reactors can be made very compact due to their inherently high energy density. Finally, the biggest advantage is the capability to rapidly switch on and off, as discussed below.

Plasma is a partially or fully ionized gas, obtainable under atmospheric conditions by, for example, applying a potential difference to a gas. The ionized mixture is highly reactive, consisting of ions, electrons, photons, atoms, radicals, and excited states.[8] Plasmas are operated in a wide range of conditions (temperature, pressure, gas ionization degree, etc.), which ultimately define the type of plasma. Based on this, plasmas are commonly divided into equilibrium (thermal) and nonequilibrium (nonthermal) plasmas. Unlike nonequilibrium plasmas, where the temperature of the gas (typically hundreds of K) is lower than the electron temperature by up to several orders of magnitude, equilibrium plasmas imply the same kinetic energy for the bulk gas and electrons (in the order of 10^4−10^5 K). Recently, an additional type of plasma, a "warm" plasma in which the temperature of the gas is high (10^3 K) but lower than that of the electrons, has been distinguished.[9,10]

The use of plasma, a physicochemical reactive system with the potential to be powered by renewable electricity because of its turnkey properties,[5,11] has been extensively investigated for the purpose of CO_2 conversion. Recent reviews emphasized the importance of plasma chemical conversion, comparing plasma-driven chemical processes to the discovery of combustion.[12,13] A clear focus has been placed on the plasma-based manufacturing of chemicals and fuels with a low carbon footprint. Furthermore, in terms of decarbonization of the existing chemical processes, in 2018, van Rooij et al. performed a first case study for electrified CO_2 reduction to CO using plasma,[14] i.e., plasmolysis of CO_2.

A very large number of research works on CO_2 conversion by plasma are available to date, which are summarized in recent reviews on this topic.[5,15−18] More specifically, advances in CO_2 plasmolysis via gliding arc plasmas have been summarized in a recent review.[19] In brief, a variety of CO_2 plasmolysis pathways exists, including the combination of various methods coupled with catalysis, or other electricity-based methods such as electrolysis.[20] The reports describe a very wide range of process performance values. A nearly full conversion with a very high energy efficiency (EE) (up to 60%) was achieved with low-pressure plasmas.[5,16] It must be noted, however, that plasmas operated below atmospheric pressure require additional equipment with high energy costs (e.g., vacuum pumps), which limits their industrial potential.[10] In contrast, atmospheric pressure plasmas (APPs) require no additional costs associated with low-pressure equipment, although the energy efficiency values are generally lower. CO_2 plasmolysis at atmospheric pressure has been performed using various plasma types, e.g., dielectric barrier discharge (DBD), atmospheric pressure glow discharge (APGD), rotating gliding arc (RGA), gliding arc plasmatron (GAP), and microwave (MW).[18,21] The numerous research publications are unified by one notion: virtually every work discusses the need for specific upscaling methods in order to bring atmospheric plasma from the lab to industry. This entails not only a physical increase of throughput but also an economics-backed approach, which couples cost and productivity to reality. In the academic setting, this is not an easy task: works with extensive knowledge on plasma fundamentals often lack economic sense and vice versa.

In this work, the efforts on the academic side, namely, the research group PLASMANT at the University of Antwerp, and its newly created spin-off D-CRBN, are merged together. The fundamental principles of plasma reactor design and operation are paired with the necessary knowledge of scale-up economics and practical considerations for large-scale operations. We present the new, upscaled D-CRBN prototype reactor, namely, the multi-reactor gliding arc plasmatron (MRGAP), and we discuss its performance for CO_2 plasmolysis. We also address the macroeconomic picture of further developments toward the industrialization of atmospheric plasma.

2. CHOICE OF TECHNOLOGY

As mentioned above, in the field of gas and chemical conversion applications, there are several viable plasma types.[5] APPs are the most appealing for industry, as they do

https://doi.org/10.1021/acsengineeringau.3c00067
ACS Eng. Au 2024, 4, 333−344

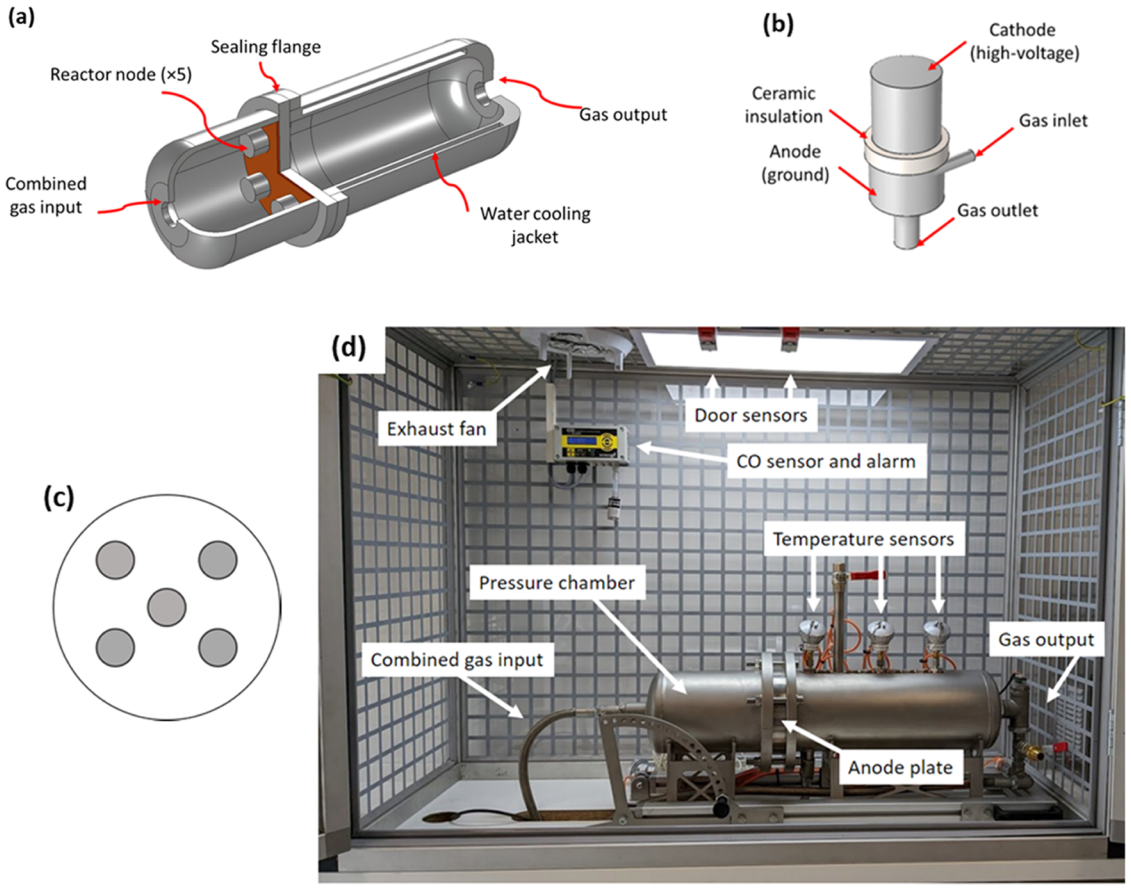

Figure 1. Multi-reactor gliding arc plasmatron (MRGAP): Schematic showing internal features (a), geometry of a single reactor node (b), anode plate configuration (c), and image of the reactor inside the fume hood (d).

not require expensive vacuum equipment and, by definition, have a higher mass throughput. Different APPs are described below.

MW plasma sources generally show good energy efficiency (EE) (over 50%), but typically at a very low pressure.[5] At atmospheric pressure, their unmodified performance (i.e., without quenching) has been shown to be similar to GA plasmas (see Table 1). Moreover, MW setups typically lead to higher capital costs, as they require complex equipment.[22] Indeed, in the paper by Detz and van der Zwaan,[23] it was mentioned that for a 20,000 t/y (CO) plant, € 21 M is the cost of the MW generators alone. They report 100% carbon efficiency, so this output equates to ca. 32,000 t/y CO_2, which corresponds to ca. 32,000 L/min. If we consider an SEI approximately equal to that of GA plasmas, we arrive at a figure of ca. 3000 kW of installed power. Thus, power supply costs can be estimated around 7000 €/kW (21 M €/3000 kW), which is somewhat higher than the total cost of our setup. The cost of our total reactor assembly, including the power supply, is currently around 3000 €/kW, for a small scale of up to 1000 t/y. This is comparable to but slightly lower than the cost for MW plasma reactors. While MW plasma setups have the advantage of not requiring the use of electrodes, other components such as waveguides and impedance tuners were not taken into account in the calculation by Detz and van der Zwaan,[23] which can further increase setup costs.

DBD plasmas have also been extensively studied for CO_2 conversion. They can operate at atmospheric pressure and can be built and upscaled at a relatively low cost. However, their conversion rate (CR) and EE are very limited (below 1 g/h, and ca. 5−10%) due to their low throughput (low flow rates), and inefficient dissociation mechanism (through electronic excitation),[5] respectively, which makes them unviable for industrial applications. APGD and RGA plasmas were also studied for CO_2 conversion and gave varied performance metrics. Some of the most recent advances in CO_2 plasmolysis using a variety of plasma reactors are summarized in Table 1.

Evidently, MW plasma processes for CO_2 conversion (Table 1, entries 1−4) generally possess the same or higher energy efficiency than other "warm" plasmas, such as APGD (entry 5), but are still predominantly operated at reduced pressures. Attempts at increasing EE at atmospheric pressure have been conducted, e.g., an active cooling of the plasma effluent (entry 2). It must be specifically noted that all data in entries 1−10 describes the performance of single reactor plasma setups. This is reflected in the low values of conversion rate (CR, see Section 5 for further discussion), which range from several sub-g/h in DBD plasma reactors (entries 6,7) to a maximum of ca. 380 g/h with MW plasma (entry 5). The low CR in the DBD is partially a consequence of the low throughput (defined by the feed gas flow rate of CO_2). Upscaling MW plasmolysis of CO_2 has been done in terms of reactor volume, which allowed high flow rates (up to 100 L/min; entry 7) but resulted in a low conversion, which leads to low CR values. In one of the most recent works, a spark-type plasma was used for CO_2 conversion.[30] However, despite the big advantage of a very low-cost power supply unit (PSU), the process metrics (i.e., EE

https://doi.org/10.1021/acsengineeringau.3c00067
ACS Eng. Au 2024, 4, 333−344

and CO_2 CR) were substantially lower than those of arc plasmas (Table 1, entry 8).

The GAP was chosen as the technology of choice for the plasma reactor presented in this work. Our previous works on CO_2 plasmolysis with GAP reactors (Table 1, entries 9 and 10) indicate that the absolute conversion and EE are on par with other plasma reactors. While the performance is not chart-topping,[32] they have a relatively simple design and can be driven with low-cost, low-complexity power supply units (PSUs): the price of the plasma setup PSUs has been identified as one of the factors hindering the wide application of APPs.[30] While classical gliding arc plasmas typically reach 5−6% of absolute conversion,[5] the more advanced reverse-vortex designs can reach ca. 10%, while maintaining a high EE of ≥25% (Table 1, entries 9 and 10). This, combined with its robust and simple construction, makes this plasma type an attractive and viable candidate for industrial applications in the field of gas processing.

3. UPSCALING METHOD

GA plasmas have been a long-time interest for plasma scientists.[33] They are a simple, robust tool, versatile with respect to important parameters, such as temperature, plasma chemistry, electrical characteristics, and so on. In the research group PLASMANT at the University of Antwerp, the technology has been studied for a variety of different reactor configurations, both experimentally,[9,34] as well as from a theoretical point of view.[35−37] However, initial attempts at design-based scaling have yielded mixed results.[9]

Looking into more detail in the literature,[38,39] it is clear that a simple physical upscaling (i.e., significantly increasing the volume of a single reactor and respectively increasing the amount of delivered power) of a gliding arc plasma reactor is not a straightforward task. The main obstacle is that the discharge should be sustained in the non-fully thermal regime (i.e., in the "warm" plasma regime). In this regime, the temperature of the gas is lower than in fully thermal mode, and the energy efficiency is at its highest[5] Thus, we chose a system of several parallel GAP reactors with 1−1.5 kW of power each, operating as a single setup. Increasing the power input per reactor would result in a plasma with all component temperatures in equilibrium (i.e., thermal plasma), which we actively avoided in the design of the MRGAP. A multi-reactor system containing several thermal plasma devices would require major alterations and additional costs to the setup. These include, but are not limited to, the requirement for active electrode cooling, increased cooling capacity post-plasma to reduce the area available for recombination reactions in addition to more regular electrode replacement due to degradation by the cathode and anode spots.

In addition to regime management, grouping several reactors into a single housing instead of operating them in parallel has advantages in both cost and build efficiency. First, a single axisymmetric anode plate and unified gas input (see Figure 1) require less complex machinery to produce than a multi-inlet lab scale device (single vs multiple axis CNC machine required). Production can also utilize standard parts, such as the copper O-rings in our setup. These O-rings are more temperature-resistant than rubber or silicone O-rings commonly used on lab-scale devices,[34] which reduces both maintenance cost and frequency.

The approach taken in relation to power supplies for the multiple gliding arcs followed the principle of parallelization; each reactor node is supplied by an individual PSU as opposed to one larger PSU driving all arcs simultaneously. This approach was elected for several reasons, primarily focused around cost and energy efficiency. First, the division of power delivery from one PSU to several reactors would require expensive division inductors, which would add another variable into the total energy efficiency of the system. Second, the individual power supply circuit of choice offers room for improvement. We believe the overall cost can drop to approximately 150 €/kW (currently around 400 €/kW) while the energy efficiency can be pushed higher than 90% (ca. 80% at the moment). The accessibility to suitable power generators with these features and the desired power rating (see below) also made this decision rather straightforward. A detailed description of the setup is presented in the following section.

4. SETUP DESCRIPTION

The pilot-scale plasma prototype used in this work, i.e., a multi-reactor gliding arc plasmatron (MRGAP), was built by D-CRBN. It consists of a unified reactor body containing five ca. 1 kW reactor nodes. Each reactor node has its own inlet, which drives vortex stabilization in the node cavity, much like in a reverse-vortex gliding arc plasmatron (GAP).[31] Key differences lie in the simplification of the geometrical features in order to accommodate faster and cheaper production.

In Figure 1a, the MRGAP prototype reactor is shown with a 1/4 cut for an internal view. Five identical gliding arc plasmatron reactors (Figure 1b) are mounted on an anode (ground) plate with a flange (Figure 1c). An insulating plate (ceramic, height = 5 mm) is used to separate the high-voltage cathodes (diameter = 18 mm, height = 19 mm) from the grounded anode (diameter = 20 mm, height = 13 mm). As shown in Figure 1d, a pressure chamber provides gas for each reactor node through a singular inlet (Figure 1a). Each reactor node has its own inlet channel (diameter = 3.2 mm), which drives its internal gas flow. Each reactor node also has its own gas outlet (diameter = 9 mm) which feeds into the larger post-plasma chamber. The pre-reactor node chamber (denoted as 'pressure chamber in Figure 1d) also holds high-voltage interconnections, which interface the nodes with their respective power supply units (PSUs). The PSUs are switching-type high voltage generators with a negative output, model GAD-1000, provided by Micro-Arc, a D-CRBN affiliated company that produces affordable PSUs for our MRGAP. These PSUs have direct advantages being very simple and low-cost, and are fine-tuned to drive arc plasmas with a power of around 1 kW DC. This is also achieved by a switching topology, which allows a current-regulated output without the need of a ballast resistor. The post-plasma chamber is also equipped with a fluid jacket for water cooling, enabled by a chiller.

The overall concept that was followed is an integrated plug-and-play module (see Supporting Information (SI), Figure S1). In simple terms, the entire setup is contained in a box with three ports: gas input, gas output, and power. The reactor, the power supplies, the diagnostics, the safety features, and the control systems are all integrated and operate together (no external plugs, and no need for any sort of reconstruction or adjustments, should the unit be relocated). The reactor is positioned inside a Faraday cage, which also acts as a fume hood. A powerful fan located on top (with a capacity of 6 m^3/

https://doi.org/10.1021/acsengineeringau.3c00067
ACS Eng. Au 2024, 4, 333−344

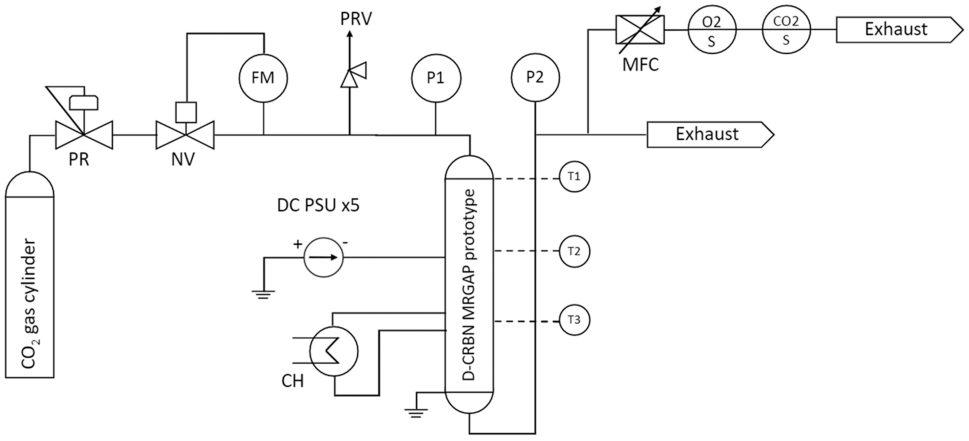

Figure 2. P&ID diagram of the setup.

min) ensures that the cage is kept at a (slightly) lower pressure compared to the lab environment.

Figure 1b shows the MRGAP setup inside the Faraday cage/fume hood. Three temperature sensors are positioned along the reactor body, as well as pressure sensors at the input and at the output gas lines. The fume hood cage is equipped with a CO sensor/alarm that shuts down operation if the internal concentration reaches 300 ppm (indicative of a leak downstream). Likewise, interlock sensors on the doors shut down the power to the reactors if the door is opened during the operation. The temperature sensors are K-type thermocouples with a limit of 1500 °C. Each sensor and control device is connected directly to the PLC (Programmable Logic Computer), which is simply an industrial PC with the options to interface with various analogue and digital I/O cards.

In Figure 2, a piping and instrumentation diagram (P&ID) is shown. The output pressure of a gas cylinder containing industrial-grade CO_2 is controlled by a pressure-reducing valve (PR). At the input of the prototype, there is a motorized needle valve (NV) that is controlled by the PLC for remote control of the flow meter (FM). The system operates in a manner similar to that of a traditional mass flow controller with the exception that the flow measurement and control features are not built into the same housing. This method of flow control has the key advantages of a lower component cost, making it more suitable for scale-up applications and compatibility with the analogue output cards of the PLC. It also allows for rapid response of the flow meter valve (because of the strong stepped motor, it reacts much faster than a typical MFC). Two pressure sensors P1 and P2 record the input and output pressure. A pressure relief valve (PRV) prevents pressure buildup (above 5 bar). The current-source type PSUs are connected in parallel to the respective reactor nodes, 5 in total. Temperature sensors T1 and T3 are indicated. The chiller (CH) is connected to the water jacket of the reactor.

For the experimental investigation presented in this work, the exhaust of the reactor is split into two parts. One is controlled by an MFC and supplies the effluent mixture into the analytical sensors O2S and CO2S (see Section 5); the other part is sent to the exhaust.

5. EXPERIMENTAL DESCRIPTION

As mentioned above, the scaled-up reactor consists of five individually powered gliding arc plasmatron (GAP) reactors operated in parallel, housed within a single reactor unit (MRGAP; see Figure 1a). Within the upscaled reactor, a grounded anode plate aligns the outlet for each individual plasmatron in a honeycomb manner. A total flow rate of 30−80 L/min of CO_2 (99.7 vol %, Air Liquide) is supplied into the MRGAP with a flow meter (SD5600, IFM Electronic) equipped with a motorized needle valve controlled from a PLC. The flow is further divided among the individual plasmatrons and fed in a tangential manner to the chambers via individual inlets (diameter = 3.2 mm). These tangential inlets generate a swirling flow within the individual reactors, stabilizing the arcs and preventing contact with the walls. We explicitly note that regardless of the number of active reactors, the combined feed gas flow rate (Figure 1a) is split between all reactors. This is done to evaluate the feasibility of changing the process input power (i.e., the reported combined SEI of the MRGAP) to compensate for the possible changes in renewable energy delivery. The flow rate of the feed gas per each of the five reactors is identical in the absence of plasma ignition (i.e., without active reactors). With any number of active reactors, a high-temperature plasma discharge will result in a decreased flow rate through those active reactors due to an increase in pressure (in accordance with the ideal gas law). However, this does not affect the calculated metrics (SEI, conversion, etc.), as they are reported for the whole MRGAP system. Each plasmatron is driven by using a DC switching-type high voltage generator (GAD-1000, Micro-Arc). The total power consumption was measured by using a three-phase power meter (iEM3150, Schneider Electric), accounting for the overall power consumed by the process. The post-plasma chamber was cooled by means of a water-cooled fluid jacket connected to a chiller (DZ5000LS-QX, Vevor). The gas temperature was recorded using K-type thermocouples at three locations along this chamber, i.e., close to the anode plate, close to the exhaust, and one in-between the two, as shown in Figures 1b and 2. The effluent of this chamber was split in two, with one part controlled by a low-ΔP mass flow controller (MFC) set to 0.8 L/min, which ensures a flow rate mixture of analytes sufficient for the sensors used. Specifically, we used an optical oxygen sensor (FDO2, PyroScience GmbH) and an NDIR CO_2 sensor (FlowEvo, SmartGas GmbH), indicated as the O2S and the CO2S in Figure 2. These sensors enable simultaneous real-time analysis of both produced O_2 and unconverted CO_2 in the gas mixture. Both sensors are for 0−100 vol % of the respective gas. Prior to each set of measurements, the sensors were calibrated individually.

The formulas used to represent and analyze the data are taken from recently updated and clarified definitions in a publication by PLASMANT.[40] Specific attention is put into the metrics calculation, which considers expansion of CO_2 due to the overall stoichiometry of the reaction (R1). In a simplified chemical pathway, CO_2 is split into CO and atomic O (R2), with the latter recombining into O_2 (R3). We explicitly mention that we did not observe the formation of solid carbon under any experimental conditions studied here. Hypothetically, C could be formed via further plasmolysis of CO (R4) but did not occur here. This clearly indicates that the temperature in our

https://doi.org/10.1021/acsengineeringau.3c00067
ACS Eng. Au 2024, 4, 333−344

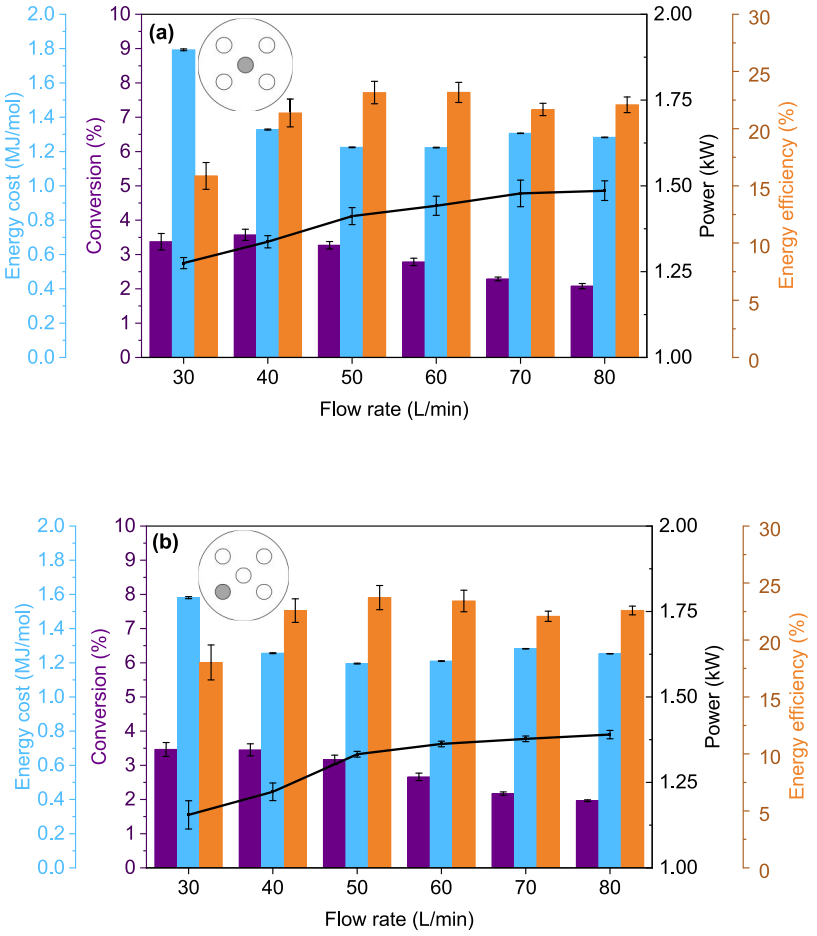

Figure 3. Energy cost, conversion, power, and energy efficiency of one active central reactor (a), and one outer reactor (b) (shown inset) as a function of the feed gas flow rate.

plasma setup was lower than that required for carbon formation (6000 K[41]).

$$CO_2 \rightleftharpoons CO + \frac{1}{2}O_2 \quad \text{(R1)}$$

$$CO_2 \rightleftharpoons CO + O \quad \text{(R2)}$$

$$O + O \rightleftharpoons O_2 \quad \text{(R3)}$$

$$CO \rightleftharpoons C + O \quad \text{(R4)}$$

The measured CO_2 concentration can be represented as the CO_2 concentration in the reactor exhaust ($\gamma^{out}_{CO_2}$) (eq 1), where n is the molar flow rate into or out of the reactor, with the superscript indicating whether this is at the inlet or outlet. This is further used to obtain the absolute conversion of CO_2 (eq 2): $\chi_{(CO_2)}$ is the conversion of CO_2, based on the measured concentration of CO_2.

$$\gamma^{out}_{CO_2} = \frac{n^{out}_{CO_2}}{n^{in}_{CO_2}} = \frac{1-\chi}{1+\frac{\chi}{2}} \quad (1)$$

$$\chi_{(CO_2)} = \frac{1-\gamma^{out}_{CO_2}}{1+\frac{\gamma^{out}_{CO_2}}{2}} \quad (2)$$

A similar derivation can be carried out for the calculation of the other reaction products, in this case O_2. $\chi_{(O_2)}$ is the conversion of CO_2 based on the measured concentration of O_2 (eq 3). We explicitly note that for every single experiment reported in this work, the shown conversion values are averages between the two conversion values obtained from the CO_2 measurement and O_2 measurement (eq 4). This was done to reduce the potential error due to the inherent uncertainty of the sensors.

$$\chi_{(O_2)} = \frac{2 \times \gamma^{out}_{O_2}}{1-\gamma^{out}_{O_2}} \quad (3)$$

$$\chi\ (\%) = \frac{\chi_{(CO_2)} + \chi_{(O_2)}}{2} \times 100\% \quad (4)$$

The energy efficiency (η) of the process, compared to the standard reaction enthalpy (ΔH^0 = +283 kJ/mol) for CO_2 dissociation, is defined as shown in eq 5, where χ is the conversion, Q^{in}_{total} is the total feed gas flow rate into the reactor, P is the power consumed during the process, and 23.6 L/mol is the molar volume of the gas at 17 °C (as calibrated by the manufacturer). In our case, the power is represented by the total power consumed from the plug as previously indicated.

$$\eta\ (\%) = \frac{\chi\ (\%) \times 283\ (\text{kJ/mol}) \times Q^{in}_{total}\ (\text{L/min})}{P\ (\text{kW}) \times 23.6\ (\text{L/mol}) \times 60\ (\text{s/min})} \quad (5)$$

The ratio of power to total molar flow rate into the reactor is another useful metric, defined as the specific energy input (SEI), expressed in kilojoules per liter, as shown in eq 6. From this ratio, the amount of energy consumed by the entire process can be defined as the energy cost (EC, MJ/mol) of the process (eq 7).

$$\text{SEI (kJ/L)} = \frac{P\ (\text{kW}) \times 60\ (\text{s/min})}{Q^{in}_{total}\ (\text{L/min})} \quad (6)$$

https://doi.org/10.1021/acsengineeringau.3c00067
ACS Eng. Au 2024, 4, 333−344

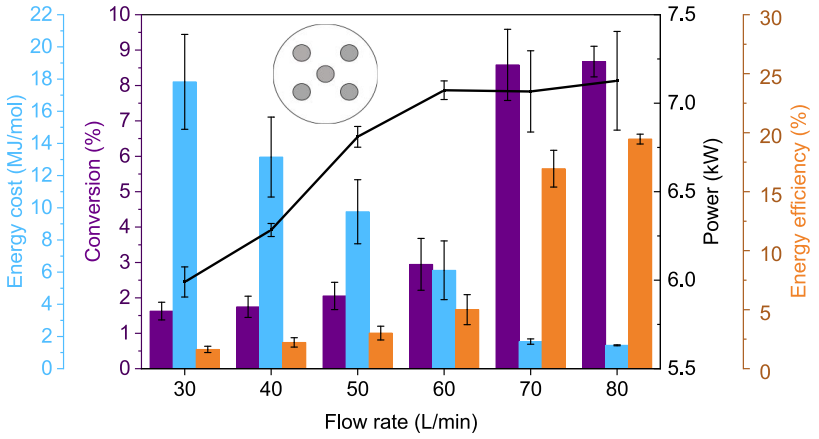

Figure 4. Energy cost, conversion, power, and energy efficiency of five active reactors (shown inset) as a function of the feed gas flow rate.

$$\mathrm{EC\ (MJ/mol)} = \frac{\mathrm{SEI\ (kJ/L)} \times 23.6\ \mathrm{(L/mol)} \times 100\%}{\chi\ (\%) \times 10^3\ \mathrm{(kJ/MJ)}} \quad (7)$$

The conversion rate (CR) is calculated as follows:

$$\mathrm{CR\ (g/h)} = \frac{Q_{\mathrm{total}}^{\mathrm{in}}\ \mathrm{(L/min)} \times \chi\ (\%) \times 60\ \mathrm{(min/h)} \times 44\ \mathrm{(g/mol)}}{23.6\ \mathrm{(L/mol)} \times 100\%} \quad (8)$$

Each experimental condition was repeated in triplicate, with the error bars shown representing the standard deviation of the gathered data.

6. RESULTS AND DISCUSSION

We examined the effect of increasing flow rate (30−80 L/min) for different configurations (see graph insets) and numbers of active reactors (1, 3, 4, 5). It must be noted that in all experiments, the flow was divided between all reactors, i.e., even with one active reactor (Figure 3) the total flow was going through all reactors, even the nonactive ones. This was done, as the specific aim of this work is to investigate the overall MRGAP performance rather than the performance of the individual GAP reactors within it. Likewise, the metrics of EC and SEI are reported for the complete setup and are based on the overall flow rate and power, as is also indicated in Table 1. Nonetheless, the flow going through each individual reactor within the MRGAP increased when the total feed gas flow increased. The power was observed to increase nearly linearly across all cases as a function of increasing flow rate. The higher flow rate likely results in both arc elongation[42] and increased resistivity,[43] resulting in an increased voltage drop across the plasma in accordance with Ohm's law. As power is the product of the applied current and voltage, this increased voltage (at a constant current) results in higher power deposition into the reactor. In all of the following plots, the conversion and energy efficiency use the same axis scale for ease of comparison between figures, whereas the energy cost and power scales are fixed within a set of active reactors for ease of interpretation.

In both configurations with one active reactor (Figure 3a,b), increasing the flow rate from 30 to 80 L/min results in a gradual decrease in CO_2 conversion, from around 3.4% to 2% between 30 and 80 L/min. The energy efficiency of the process follows a contrary trend, increasing from around 17% (at 30 L/min) to a relatively constant value around 23% (for flow rates above and including 40 L/min). The power in both instances increased by a factor of 1.2 between 30 and 80 L/min in a near-linear manner. The energy cost of the process initially decreases from ca. 1.7 MJ/mol at 30 L/min as a function of increasing flow rate, reaching a steady minimal value around 1.2 MJ/mol for the flow rates in the range of 40 to 80 L/min. The highest conversion obtained with a single active reactor occurred at the lowest investigated flow rate, 30 L/min. At higher flow rates, the fraction of gas passing through and being treated by the plasma decreases, resulting in the observed downward trend in conversion. This phenomenon has been more thoroughly experimentally investigated in previous works investigating CO_2 splitting in warm plasma setups.[8,44] The observed decrease can be framed by the fact that the "effective SEI", that is, the ratio of power to gas treated by the plasma, is not constant as a function of increasing flow rate (i.e., power and flow rate increases are not directly proportional). Despite this decreasing trend in conversion, the energy efficiency rises to a maximum value of 24% at 50 L/min. Above 40 L/min, in both configurations, this value remains relatively constant, around 22−23%. This remains relatively constant as the decrease in conversion is balanced by the ratio of flow rate to power supplied to the process (i.e., the inverse of SEI); in other words, the conversion drops at the same rate as the drop in SEI; see eqs 5 and 6.

In the SI, we plot the energy cost, conversion, power, and energy efficiency of both three and four active reactors at several different positions; see Figures S1 and S2 and detailed description in the SI.

Interestingly, for a given number of active reactors, the spatial configuration does not appear to impact the performance. Conversion, EE, and EC values remain similar regardless of the location of the GAP reactors within the MRGAP reactor plate (see Figures 3a,3b, S1a,b, and S2a,b). This could be seen as counterintuitive: to maintain the size of the overall setup within reasonable dimensions, the GAPs are positioned in a close range to each other, which suggests that the effluents of individual GAP reactors could interact with one another, leading to changes in the overall process performance. However, this is not the case, as is evident from the results. This indicates that the upscaling carried out in this work is straightforward, simplified by the reduced interference of individual reactors on each other.

The most industrially relevant and interesting results were obtained for the flow rate variation analysis carried out with five active reactors (Figure 4). Once again, the peak-like

https://doi.org/10.1021/acsengineeringau.3c00067
ACS Eng. Au 2024, 4, 333−344

behavior for conversion can be observed, moving from a low value of 1.6% at 30 L/min (post-plasma chamber temperature ca. 600 °C) to a maximum of 8.7% at 80 L/min (at a lower post-plasma gas temperature, ca. 440 °C). Promisingly, the energy efficiency for this configuration rises from 1.6% at 30 L/min to reach a maximum value of ca. 20% at 80 L/min, corresponding to the optimal conversion of 8.7% (see also Table 1, entry 11, in Section 2). The total power deposited in the system once again increases by a factor of 1.2 between the lowest and highest investigated flow rates, from 6 kW at 30 L/min to 7.1 kW at 80 L/min. As observed with four active reactors (see Figure S2a,b in the Supporting Information), the energy cost of the process follows an inverse trend to that observed for conversion under these conditions, decreasing from 17.8 MJ/mol at 30 L/min to a minimum value of 1.5 MJ/mol at 80 L/min. The maximal conversion obtained with all five active reactors is the highest among all investigated conditions and configurations, highlighting the synergistic effect between flow rate and number of active reactors (and hence plasma-deposited power). The conversion at lower flow rates is likely affected by the post-plasma chamber gas temperature being too high, which leads to an increased recombination reaction rate (due to the temperature dependence[45]), resulting in the produced CO and O_2 recombining into CO_2 (as also observed at low flow rates with three and four active reactors; see Supporting Information: Figures S1 and S2). This issue in CO_2 conversion is a topic of research in the plasma community, primarily focused on the quenching of these recombination reactions by rapidly cooling the effluent, either conductively (heat transfer to cooled walls[25]) or convectively (supersonic nozzles).[24,26]

In summary, all data presented in Figures 3, 4, S1, and S2 reveals that the trend of CO_2 conversion in all cases has a peak maximum, but this maximum is shifted from the lower flow rates with one active reactor toward higher flow rates with five active reactors. This is attributed to two factors: (i) a small number of active reactors at high flow rates means a lower fraction of plasma-treated gas and (ii) thermal effects, where higher temperature (reached at lower flow rates with the increasing number of reactors) promotes recombination of CO with O/O_2 into CO_2. Although our current available infrastructure limited the investigation to flow rates not exceeding 80 L/min, a further study with higher flow rates is planned for future work.

Under optimized conditions (five active reactors and 80 L/min CO_2 feed), we achieved a process performance with ca. 9% CO_2 conversion, 20% energy efficiency, an energy cost of 1.5 MJ/mol CO_2, and an exceptional CO_2 conversion rate of nearly 780 g/h (see Table 1, entry 11), which is of industrial interest. While these EE and EC values appear lower than most values presented in Table 1, we should emphasize that these values are calculated based on the plug power. This is uncommon in publications found in the literature, where the energy metrics are calculated based solely on plasma-deposited power. While the latter approach is more informative for fundamental studies, we infer that industry-oriented research should focus on the total plug power, such as the one reported in this work. To enable direct comparison between the values obtained here and those found in the literature, we measured the energy efficiency of our PSUs, i.e., the efficiency of converting plug power into plasma-deposited power. The values were found to be ca. 77−83%. Thus, with a reasonable approximation of the energy efficiency being 80%, the EE and EC values based on plasma-deposited power become 24% and 1.2 MJ/mol—very close to the best values shown in Table 1.

A useful method for comparing data with varying power inputs (such as in the case with more or fewer active reactors) is plotting conversion as a function of SEI. The most ideal conditions should yield high conversion values for a low SEI value. As the SEI is essentially the ratio of power input to flow rate, increasing SEI can be the result of either higher power input (at constant flow rate) or lower flow rate (at constant power input). In reality, as observed in Figures 3, 4, S1, and S2, increasing flow rate results in increasing power deposition. In this instance, an increasing SEI value can be interpreted as the relative change in power being larger than the relative change in flow rate between steps and vice versa.

The collected data shown in Figure 5a reveals that an optimal SEI value exists for the peak conversion of CO_2. This peak corresponds to approximately 5.3 kJ/L regardless of the

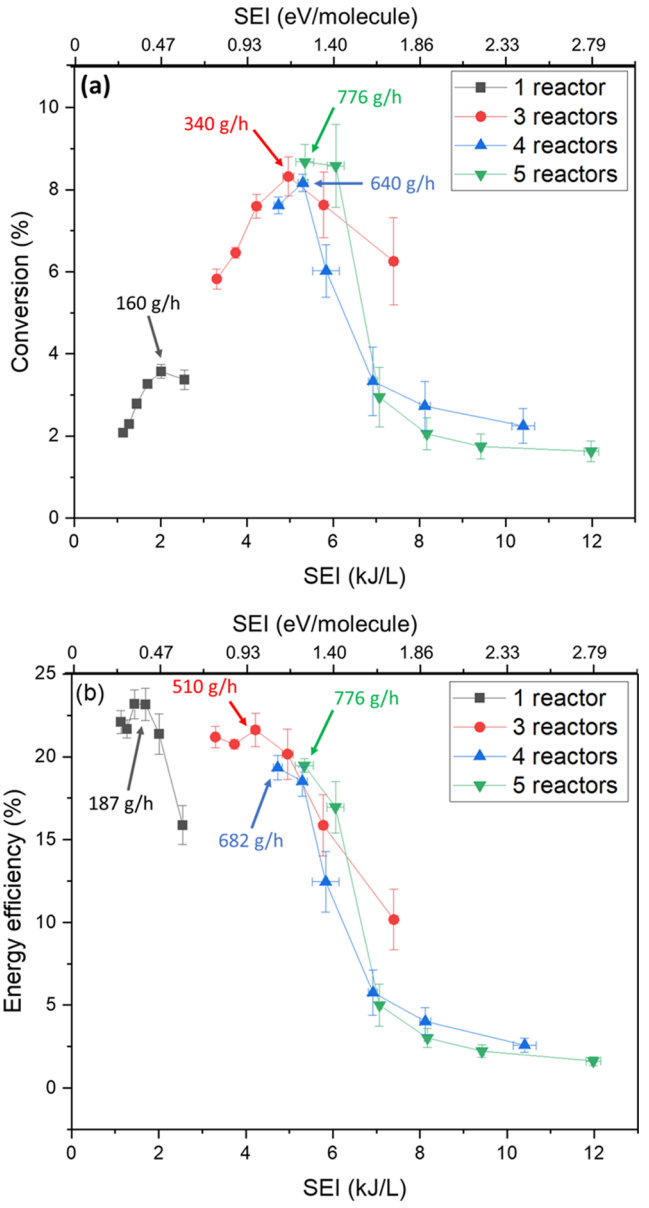

Figure 5. CO_2 conversion (a) and energy efficiency (b) as functions of the specific energy input. The reactor configuration was the same as that shown in Figure 6b.

https://doi.org/10.1021/acsengineeringau.3c00067
ACS Eng. Au 2024, 4, 333−344

number of active reactors (3, 4, or 5). This peak indicates that to obtain optimum conversion an ideal ratio between the power deposited into the system and the flow rate should be reached. However, while the same conversion can be reached at this SEI value for different configurations, the conversion rate (CR) differs greatly (see Figure S3 in the SI for plot of conversion rate as a function of increasing flow rate and number of active reactors). Around this peak SEI value of 5.3 kJ/L, the CR for three active reactors is 340 g/h, compared to 777 g/h with five active reactors. This relationship implies that parallelization of reactors within a single unit is only limited by the amount of power and feed flow rate supplied, demonstrating the success of our upscaling approach.

While 777 g/h corresponds to 6.7 t/y of converted CO_2, further increasing both the number of active reactors (hence power) and flow rate, while remaining around this SEI value of 5.3 kJ/L, should result in an increase in conversion rate. Of course, the current iteration of the prototype would require massive upscaling to meet industrial demands. Hence, further optimizations to the MRGAP are required. Such alterations include changing the electrode design to accommodate higher flow rates or using a post-plasma carbon bed to scavenge the oxygen and further improve conversion. The latter has been demonstrated to work on a lab scale,[31,46] and is currently being investigated for the MRGAP.

In terms of energy efficiency as a function of the SEI, a different trend is observed in Figure 5b. With one active reactor, the best energy efficiency is obtained for the lowest SEI (23% at 1.4 kJ/L). However, the CR at these conditions (187 g/h) is too low to be of industrial interest. With more active reactors, a peak in energy efficiency emerges around 5.3 kJ/L. Further increasing the SEI only decreases the efficiency of the process, providing too much power into the system. While the best efficiency is obtained around this value with 3 active reactors (ca. 21% for an SEI of 4.2 kJ/L), the CR at this condition is still lower (510 g/h) than with more active reactors. For an energy efficiency of ca. 20%, five active reactors convert 777 g/h at an SEI of 5.3 kJ/L. In other words, a decrease in EE by a factor of 1.15, allows the CR to increase by a factor of 4.15. In terms of scaling up technology, the benefit of a largely increased CR evidently outweighs the minor losses made in energy efficiency.

In the context of current literature, D'Isa et al.[8] obtained similar conversion and energy efficiency trends as a function of SEI in their quasi-atmospheric, unmodified microwave plasma setup. As they were able to vary the power and the flow rate significantly, they were able to scan a wide SEI range, which revealed these trends. At several different flow rate conditions, they observed a peak in conversion at an SEI value around 2 eV/molecule (ca. 8.6 kJ/L). As for energy efficiency, they also initially observed a relatively constant energy efficiency as a function of increasing the SEI, followed by a decrease at higher values. In comparison to CO_2 conversion experiments carried out in a single GAP reactor by Ramakers,[47] their conversion results align with those obtained for the single active reactor case in our work. An increase in SEI results in increased conversion, up to 6% at an SEI value of around 4 kJ/L (1 eV/molecule). Interestingly, this value lies in the region of the estimated plasma-based optimum SEI obtained in our current study (ca. 4.2 kJ/L, Table 1).

7. ECONOMICS OF SCALING

As previously discussed, the upscaling principle used by D-CRBN for the MRGAP prototype is based on parallelization with a limited window of power and flow rate supply per reactor, in order to maintain the "warm" plasma regime. This is also closely related to the reactor dimensions, as demonstrated in other works.[32] On the economic side, this makes a significant difference to the way in which a project can be scaled up.

An example of the cost per installed capacity is shown in Figure 6. Q1 is the stage wherein a proof-of-concept (POC) system is shown. This is typically a high-cost, low-capacity unit demonstrating the technology, which carries over heavy costs from the research phase. In Q2, we have a pilot or demo-scale system, which works at an increased capacity but no longer bears the costs of research. The main costs in this period are related to product engineering. In Q3, the industrial stage is reached, and the cost of a given system can be as low as the total amount spent developing Q1. However, this cost comes with a vastly increased capacity, backed by market acceptance and a working business model. The main cost is large-scale manufacturing. In this final phase, the cost per capacity may increase slightly (cf. Figure 6) due to costs incurred from the streamlining of manufacturing.

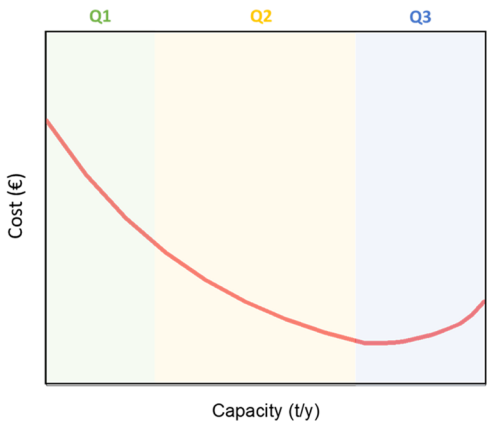

Figure 6. Typical cost-per-capacity dependence, starting from high-cost low-capacity (Q1), and moving toward low-cost, high-capacity (Q2-Q3).

A parallel can be made with the development of the transistor, which was footed on a long and expensive research phase, for a single, lab-scale device, in 1947.[48] In 1958, Fairchild sold its first batch of marketed transistors for $150 each.[49] Currently, transistors are probably the least expensive device ever produced industrially, as billions are situated in nearly every modern chip. Economies of scale are a complex matter, deeply rooted in concepts of management, trading, and sociology, but in general, it is known that costs go down due to the following main factors: (i) expansion of the industry or the market; (ii) increase of purchasing power; (iii) governmental initiatives, i.e., politics.

The scaling formula for multiplication is shown in eq 9,[47] where C_2 is the final cost of the equipment, C_1 is the initial cost, and N is the number of units that are built.

$$C_2 = C_1 \times N^{0.9} \tag{9}$$

If we apply this formula for a few starting cost levels and scale them for different capacities, we get the following figure:

https://doi.org/10.1021/acsengineeringau.3c00067
ACS Eng. Au 2024, 4, 333−344

The capital expenditure (CAPEX) per installed kW for our setup currently lies at around €3000. However, it should be noted that CAPEX does not fully represent the economic viability of a project focused on the scaling up of a technology. When planning the upscaling, it must be calculated together with the operational expenditure (OPEX), interest rate, amortization, and taxes to construct a valid total cost of ownership (TCO) prediction. All of this information is then included in a net present value (NPV) based on which investment decisions are made. While this complete calculation is of economic interest, it is currently outside the scope of this work.

With the aim of achieving a conversion capacity of 1 Mt of CO_2 per year (*i.e.*, 10^6 t/y in Figure 7) in a single plant, the cost for such a plant would be around 600 €/kW. Of course, this is a gross simplification: not every component in the system will be governed by eq 9. Pressure tanks, storage vessels, buffers, and various support structures will benefit from a much greater capital impact, as they are upscaled in terms of volume rather than multiplication. For these entities, the following equation is applied, which is the general law of linear upscaling (eq 10)[50]

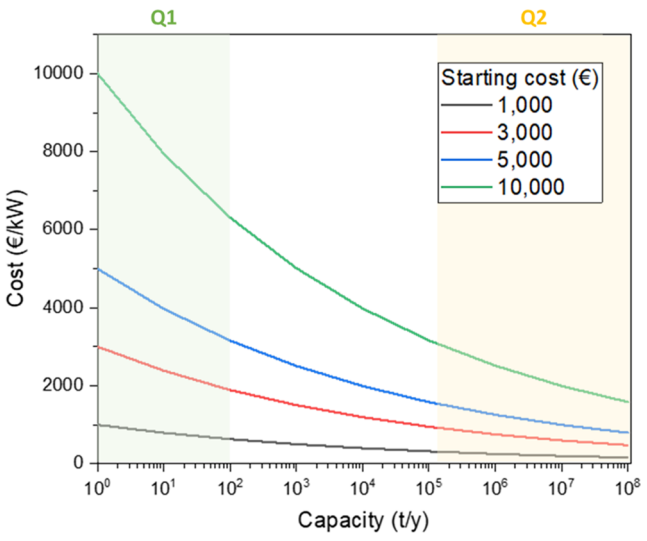

Figure 7. Cost train per installed kW as a function of capacity for a few (arbitrary) starting costs.

$$C_2 = C_1 \times \left(\frac{\text{size}_2}{\text{size}_1}\right)^{0.6} \quad (10)$$

The combination of eqs 9 and 10 results in a significantly lower cost per installed capacity. These equations are derived empirically and are generally assumed to be reasonably accurate for most economic models. A more complete and accurate overview of the business costs requires an in-depth model, which can be obtained by using specific software, such as Aspen Plus.

In addition to a more in-depth business cost analysis, it should also be noted that a cost for separating $CO_2/CO/O_2$ (*i.e.*, CO_2 splitting products when full conversion is not achieved) should also be accounted for in a total cost evaluation. However, this is outside the scope of this work and highly dependent on the location of the integrated system, where there will be technical, geographical, and economical constraints.

8. CONCLUSIONS

In this work, we have presented a successful method for the scaling of atmospheric pressure warm plasma sources, namely, the parallelization of gliding arc plasmatron reactors within a singular reactor unit. We investigated the effect of varying the number of active reactors (1, 3, 4, and 5) as a function of total feed gas flow rate (30−80 L/min).

A peak-like behavior was observed in the conversion of CO_2, which shifted toward higher flow rates with increasing the number of active reactors. With a single active reactor, increasing the flow rate resulted in lower conversion. This decrease is ascribed to the fact that the power did not increase proportionally to the flow, which resulted in less of the input gas passing through and being treated by the plasma. With three active reactors, this effect was also observed on the right-hand side of the conversion peak at the highest flow rate. To the left of this peak, i.e., at low flow rates, the post-reactor chamber gas temperature was not lowered sufficiently (either temporally or spatially) by either the cold gas stream or the water-cooled walls, resulting in low conversion due to the temperature-dependent recombination of CO with O/O_2 to form CO_2 again. Five active reactors only showed the left-hand side of the conversion peak, reaching a maximal conversion (8.7%) at the highest investigated feed gas flow rate (80 L/min).

Our results evidence that an optimum conversion of around 9% can be achieved with varying numbers of active reactors (3−5). This conversion occurs at a specific ratio between power and feed gas flow rate (i.e., SEI), around 5.3 kJ/L of CO_2. While the CO_2 conversion at this SEI value for different configurations was approximately equal, operating five reactors in parallel resulted in the highest conversion rate (777 g/h) for all conditions studied.

This work clearly shows that operating multiple single gliding arc plasmatrons in parallel in a singular reactor unit is a viable method for plasma technology scale-up with regard to CO_2 utilization. In future work, we plan to investigate higher flow rate conditions (>80 L/min), in addition to operating more reactors in parallel.

In addition to the experimental work, we also elaborate on an important aspect of industrial transition: upscaling. The results indicate that the method of upscaling using the principle of operating parallelized plasmatrons within a single unit can be successful. The overall reactor performance is preserved from the lab-scale level as evidenced by the metrics (see Table 1). Moreover, safety features and utilities required by the industry are implemented and demonstrated. In this way, D-CRBN has mitigated the risks on the pathway toward pilot-scale developments, ensuring fundamentally safe operation while remaining flexible for the changing industrial demands.

■ ASSOCIATED CONTENT

Supporting Information

The Supporting Information is available free of charge at https://pubs.acs.org/doi/10.1021/acsengineeringau.3c00067.

Energy cost, conversion, power, and energy efficiency for three and four active reactors; CO_2 conversion rate as a

https://doi.org/10.1021/acsengineeringau.3c00067
ACS Eng. Au 2024, 4, 333−344

function of feed gas flow rate for various reactor configurations (PDF)

AUTHOR INFORMATION

Corresponding Author

Yury Gorbanev − *Research Group PLASMANT, Department of Chemistry, University of Antwerp, 2610 Antwerp, Belgium;* orcid.org/0000-0002-8059-4464; Phone: +32(0)32652343; Email: yury.gorbanev@uantwerpen.be

Authors

Colin O'Modhrain − *Research Group PLASMANT, Department of Chemistry, University of Antwerp, 2610 Antwerp, Belgium;* orcid.org/0000-0002-0562-4408

Georgi Trenchev − *D-CRBN, 2020 Antwerp, Belgium*

Annemie Bogaerts − *Research Group PLASMANT, Department of Chemistry, University of Antwerp, 2610 Antwerp, Belgium;* orcid.org/0000-0001-9875-6460

Complete contact information is available at: https://pubs.acs.org/10.1021/acsengineeringau.3c00067

Author Contributions

§C.O. and G.T. share first authorship. Y.G. and A.B. share senior authorship. The manuscript was written through contributions of all authors. All authors have given approval to the final version of the manuscript.

Funding

This research was financially supported by the VLAIO-Catalisti ICON project "BluePlasma" (grant ID HBC.2022.0445), as well as by the European Research Council (ERC) under the European Union's Horizon 2020 research and innovation program (grant agreement no. 810182—SCOPE ERC Synergy project, and grant agreement no. 101081162—PREPARE ERC Proof of Concept project).

Notes

The authors declare no competing financial interest.

ACKNOWLEDGMENTS

The authors thank Amira Vandenbroucke (D-CRBN, PLASMANT) for her help in gathering the experimental data and with the initial testing of the plasma reactor.

ABBREVIATIONS

APP, atmospheric pressure plasma; AC, alternating current; DC, direct current; DBD, dielectric barrier discharge; GAP, gliding arc plasmatron; APGD, atmospheric pressure glow discharge; MW, microwave; MRGAP, multi-reactor gliding arc plasmatron; EE, energy efficiency; CR, conversion rate; EC, energy cost; PSU, power supply unit; PLC, programmable logic computer; PR, pressure reducer; PRV, pressure relief valve; NV, needle valve; FM, flow meter; PS, pressure sensor; CH, chiller; MFC, mass flow controller; NDIR, nondispersive infrared (spectroscopy); SEI, specific energy input; CAPEX, capital expenditure; OPEX, operational expenditure; TCO, total cost of ownership; NPV, net present value

REFERENCES

(1) Burek, S. When will fossil fuels finally run out and what is the technical potential for renewable energy resources? *I. J. COMADEM* **2010**, *13*, 22−27.

(2) Bogdanov, D.; Ram, M.; Aghahosseini, A.; Gulagi, A.; Oyewo, A. S.; Child, M.; Caldera, U.; Sadovskaia, K.; Farfan, J.; et al. Low-cost renewable electricity as the key driver of the global energy transition towards sustainability. *Energy* **2021**, *227*, No. 120467.

(3) Genc, T. S.; Kosempel, S. Energy Transition and the Economy: A Review Article. *Energies* **2023**, *16* (7), No. 2965.

(4) Winter, L. R.; Chen, J. G. N2 Fixation by Plasma-Activated Processes. *Joule* **2021**, *5* (2), 300−315.

(5) Snoeckx, R.; Bogaerts, A. Plasma technology - a novel solution for CO_2 conversion? *Chem. Soc. Rev.* **2017**, *46* (19), 5805−5863.

(6) Chen, H.; Yuan, D.; Wu, A.; Lin, X.; Li, X. Review of low-temperature plasma nitrogen fixation technology. *Waste Disposal Sustainable Energy* **2021**, *3* (3), 201−217.

(7) Mallapragada, D. S.; Dvorkin, Y.; Modestino, M. A.; Esposito, D. V.; Smith, W. A.; Hodge, B.-M.; Harold, M. P.; Donnelly, V. M.; Nuz, A.; Bloomquist, C.; et al. Decarbonization of the chemical industry through electrification: Barriers and opportunities. *Joule* **2023**, *7* (1), 23−41.

(8) D'Isa, F. A.; Carbone, E. A. D.; Hecimovic, A.; Fantz, U. Performance analysis of a 2.45 GHz microwave plasma torch for CO_2 decomposition in gas swirl configuration. *Plasma Sources Sci. Technol.* **2020**, *29* (10), No. 105009.

(9) Vertongen, R.; Bogaerts, A. How important is reactor design for CO_2 conversion in warm plasmas? *J. CO_2 Util.* **2023**, *72*, No. 102510.

(10) Adamovich, I.; Agarwal, S.; Ahedo, E.; Alves, L. L.; Baalrud, S.; Babaeva, N.; Bogaerts, A.; Bourdon, A.; Bruggeman, P. J.; Canal, C.; et al. The 2022 Plasma Roadmap: low temperature plasma science and technology. *J. Phys. D: Appl. Phys.* **2022**, *55* (37), No. 373001.

(11) Bogaerts, A.; Neyts, E. C. Plasma Technology: An Emerging Technology for Energy Storage. *ACS Energy Lett.* **2018**, *3* (4), 1013−1027.

(12) Cha, M. S.; Snoeckx, R. Plasma Technology−Preparing for the Electrified Future. *Front. Mech. Eng.* **2022**, *8*, No. 903379.

(13) Delikonstantis, E.; Cameli, F.; Scapinello, M.; Rosa, V.; Van Geem, K. M.; Stefanidis, G. D. Low-carbon footprint chemical manufacturing using plasma technology. *Curr. Opin. Chem. Eng.* **2022**, *38*, No. 100857.

(14) van Rooij, G. J.; Akse, H. N.; Bongers, W. A.; van de Sanden, M. C. M. Plasma for electrification of chemical industry: a case study on CO_2 reduction. *Plasma Phys. Controlled Fusion* **2018**, *60* (1), No. 014019.

(15) Bogaerts, A.; Centi, G. Plasma Technology for CO_2 Conversion: A Personal Perspective on Prospects and Gaps. *Front. Energy Res.* **2020**, *8*, No. 111.

(16) Ong, M. Y.; Nomanbhay, S.; Kusumo, F.; Show, P. L. Application of microwave plasma technology to convert carbon dioxide (CO_2) into high value products: A review. *J. Cleaner Prod.* **2022**, *336*, No. 130447.

(17) Ray, D.; Ye, P.; Yu, J. C.; Song, C. Recent progress in plasma-catalytic conversion of CO_2 to chemicals and fuels. *Catal. Today* **2023**, *423*, No. 113973.

(18) George, A.; Shen, B.; Craven, M.; Wang, Y.; Kang, D.; Wu, C.; Tu, X. A Review of Non-Thermal Plasma Technology: A novel solution for CO_2 conversion and utilization. *Renewable Sustainable Energy Rev.* **2021**, *135*, No. 109702.

(19) Liu, J.-L.; Wang, X.; Li, X.-S.; Likozar, B.; Zhu, A.-M. CO2 conversion, utilisation and valorisation in gliding arc plasma reactors. *J. Phys. D: Appl. Phys.* **2020**, *53* (25), No. 253001.

(20) Pandiyan, A.; Kyriakou, V.; Neagu, D.; Welzel, S.; Goede, A.; van de Sanden, M. C. M.; Tsampas, M. N. CO_2 conversion via coupled plasma-electrolysis process. *J. CO_2 Util.* **2022**, *57*, No. 101904.

(21) Zhang, H.; Li, L.; Li, X.; Wang, W.; Yan, J.; Tu, X. Warm plasma activation of CO_2 in a rotating gliding arc discharge reactor. *J. CO_2 Util.* **2018**, *27*, 472−479.

(22) Kelly, S.; Bogaerts, A. Nitrogen fixation in an electrode-free microwave plasma. *Joule* **2021**, *5* (11), 3006−3030.

(23) Detz, R. J.; van der Zwaan, B. Cost projections for microwave plasma CO production using renewable energy. *J. Energy Chem.* **2022**, *71*, 507−513.
(24) Hecimovic, A.; D'Isa, F. A.; Carbone, E.; Fantz, U. Enhancement of CO_2 conversion in microwave plasmas using a nozzle in the effluent. *J. CO_2 Util.* **2022**, *57*, No. 101870.
(25) Hecimovic, A.; Kiefer, C. K.; Meindl, A.; Antunes, R.; Fantz, U. Fast gas quenching of microwave plasma effluent for enhanced CO2 conversion. *J. CO_2 Util.* **2023**, *71*, No. 102473.
(26) Mercer, E. R.; Van Alphen, S.; van Deursen, C. F. A. M.; Righart, T. W. H.; Bongers, W. A.; Snyders, R.; Bogaerts, A.; van de Sanden, M. C. M.; Peeters, F. J. J. Post-plasma quenching to improve conversion and energy efficiency in a CO_2 microwave plasma. *Fuel* **2023**, *334*, No. 126734.
(27) Vertongen, R.; Trenchev, G.; Van Loenhout, R.; Bogaerts, A. Enhancing CO_2 conversion with plasma reactors in series and O_2 removal. *J. CO_2 Util.* **2022**, *66*, No. 102252.
(28) Yukio, H. CO_2 conversion characteristics in a micro-gap DBD plasma reactor. *Int. J. Plasma Environ. Sci.* **2023**, *17*, No. e01007.
(29) Rao, M. U.; Bhargavi, K. V. S. S.; Chawdhury, P.; Ray, D.; Vanjari, S. R. K.; Subrahmanyam, C. Non-thermal plasma assisted CO_2 conversion to CO: Influence of non-catalytic glass packing materials. *Chem. Eng. Sci.* **2023**, *267*, No. 118376.
(30) Xu, Y.; Gao, Y.; Xi, D.; Dou, L.; Zhang, C.; Lu, B.; Shao, T. Spark Discharge Plasma-Enabled CO_2 Conversion Sustained by a Compact, Energy-Efficient, and Low-Cost Power Supply. *Ind. Eng. Chem. Res.* **2023**, *62*, 15872−15883.
(31) Girard-Sahun, F.; Biondo, O.; Trenchev, G.; van Rooij, G.; Bogaerts, A. Carbon bed post-plasma to enhance the CO2 conversion and remove O2 from the product stream. *Chem. Eng. J.* **2022**, *442*, No. 136268.
(32) Kaufmann, S. J.; Rößner, P.; Renninger, S.; Lambarth, M.; Raab, M.; Stein, J.; Seithümmer, V.; Birke, K. P. Techno-Economic Potential of Plasma-Based CO2 Splitting in Power-to-Liquid Plants. *Appl. Sci.* **2023**, *13* (8), No. 4839.
(33) Fridman, A. Gliding Arc Discharge. In *Plasma Chemistry*, 1st ed.; Cambridge University Press, 2008; pp 200−207.
(34) Ramakers, M.; Trenchev, G.; Heijkers, S.; Wang, W.; Bogaerts, A. Gliding Arc Plasmatron: Providing an Alternative Method for Carbon Dioxide Conversion. *ChemSusChem* **2017**, *10* (12), 2642−2652.
(35) Sun, S. R.; Kolev, S.; Wang, H. X.; Bogaerts, A. Coupled gas flow-plasma model for a gliding arc: investigations of the back-breakdown phenomenon and its effect on the gliding arc characteristics. *Plasma Sources Sci. Technol.* **2017**, *26*, No. 015003.
(36) Kolev, S.; Bogaerts, A. Similarities and differences between gliding glow and gliding arc discharges. *Plasma Sources Sci. Technol.* **2015**, *24* (6), No. 065023.
(37) Wang, W.; Berthelot, A.; Kolev, S.; Tu, X.; Bogaerts, A. CO2 conversion in a gliding arc plasma: 1D cylindrical discharge model. *Plasma Sources Sci. Technol.* **2016**, *25* (6), No. 065012.
(38) Fridman, A. *Plasma Chemistry*; Cambridge University Press: New York, 2009 978−1107684935.
(39) Rabinovich, A.; Nirenberg, G.; Kocagoz, S.; Surace, M.; Sales, C.; Fridman, A. Scaling Up of Non-Thermal Gliding Arc Plasma Systems for Industrial Applications. *Plasma Chem. Plasma Process.* **2022**, *42* (1), 35−50.
(40) Wanten, B.; Vertongen, R.; De Meyer, R.; Bogaerts, A. Plasma-based CO2 conversion: How to correctly analyze the performance? *J. Energy Chem.* **2023**, *86*, 180−196.
(41) Centi, G.; Perathoner, S.; Papanikolaou, G. Plasma assisted CO2 splitting to carbon and oxygen: A concept review analysis. *J. CO_2 Util.* **2021**, *54*, No. 101775.
(42) Tsonev, I.; O'Modhrain, C.; Bogaerts, A.; Gorbanev, Y. Nitrogen Fixation by an Arc Plasma at Elevated Pressure to Increase the Energy Efficiency and Production Rate of NOx. *ACS Sustainable Chem. Eng.* **2023**, *11* (5), 1888−1897.
(43) Trenchev, G.; Kolev, S.; Wang, W.; Ramakers, M.; Bogaerts, A. CO2 Conversion in a Gliding Arc Plasmatron: Multidimensional Modeling for Improved Efficiency. *J. Phys. Chem. C* **2017**, *121* (44), 24470−24479.
(44) van den Bekerom, D. C. M.; Linares, J. M. P.; Verreycken, T.; van Veldhuizen, E. M.; Nijdam, S.; Berden, G.; Bongers, W. A.; van de Sanden, M. C. M.; van Rooij, G. J. The importance of thermal dissociation in CO2 microwave discharges investigated by power pulsing and rotational Raman scattering. *Plasma Sources Sci. Technol.* **2019**, *28* (5), No. 055015.
(45) Tsang, W.; Hampson, R. F. Chemical Kinetic Data Base for Combustion Chemistry. Part I. Methane and Related Compounds. *J. Phys. Chem. Ref. Data* **1986**, *15* (3), 1087−1279.
(46) Liu, P.; Liu, X.; Shen, J.; Yin, Y.; Yang, T.; Huang, Q.; Auerbach, D.; Kleiyn, A. W. CO2 conversion by thermal plasma with carbon as reducing agent: high CO yield and energy efficiency. *Plasma Science and Technology* **2019**, *21* (1), No. 012001.
(47) Ramakers, M. *Using a Gliding Arc Plasmatron for Carbon Dioxide Conversion - The Future in Industry?*, Universiteit Antwerpen, 2019.
(48) Puers, R.; Baldi, L.; Van de Voorde, M.; van Nooten, S. E. *Nanoelectronics: Materials, Devices, Applications*; Wiley, 2017; Vol. 2.
(49) 1958: Silicon Mesa Transistors Enter Commercial Production. https://www.computerhistory.org/siliconengine/silicon-mesa-transistors-enter-commercial-production/. (accessed October 12, 2023).
(50) Towler, G.; Sinnott, R. *Chemical Engineering Design: Principles, Practice and Economics of Plant and Process Design*; Elsevier, 2008.

https://doi.org/10.1021/acsengineeringau.3c00067
ACS Eng. Au 2024, 4, 333−344